4214–4222 *Nucleic Acids Research, 2007, Vol. 35, No. 12* *Published online 18 June 2007*
doi:10.1093/nar/gkm316

Intramolecular DNA quadruplexes with different arrangements of short and long loops

Phillip A. Rachwal[1], I. Stuart Findlow[1], Joern M. Werner[1], Tom Brown[2] and Keith R. Fox[1,*]

[1]School of Biological Sciences, University of Southampton, Bassett Crescent East, Southampton SO16 7PX, UK and [2]School of Chemistry, University of Southampton, Highfield, Southampton SO17 1BJ, UK

Received March 10, 2007; Revised and Accepted April 13, 2007

ABSTRACT

We have examined the folding, stability and kinetics of intramolecular quadruplexes formed by DNA sequences containing four G_3 tracts separated by either single T or T_4 loops. All these sequences fold to form intramolecular quadruplexes and 1D-NMR spectra suggest that they each adopt unique structures (with the exception of the sequence with all three loops containing T_4, which is polymorphic). The stability increases with the number of single T loops, though the arrangement of different length loops has little effect. In the presence of potassium ions, the oligonucleotides that contain at least one single T loop exhibit similar CD spectra, which are indicative of a parallel topology. In contrast, when all three loops are substituted with T_4 the CD spectrum is typical of an antiparallel arrangement. In the presence of sodium ions, the sequences with two and three single T loops also adopt a parallel folded structure. Kinetic studies on the complexes with one or two T_4 loops in the presence of potassium ions reveal that sequences with longer loops display slower folding rates.

INTRODUCTION

DNA sequences that contain four or more closely spaced G-tracts can fold to form intramolecular quadruplexes, which consist of stacked G-quartets that are linked by three loops between the four G-strands (1–4). These structures are stabilized by monovalent cations (especially potassium) (5,6) and can adopt a variety of different folding patterns dependent on the relative orientation of the strands and the position of the loops. G-rich sequences with the potential to form quadruplex structures are common in genomic DNA and these have been identified in several biologically important regions (7–9). The most widely studied is telomeric DNA, which in higher eukaryotes is composed of repeats of the sequence GGGTTA (10,11) and for which about 50–100 bases at the 3′-end are single stranded. A number of other non-telomeric G-rich DNA sequences may also form quadruplexes and these have been identified in the promoters of *c-myc* (12–15), Ki-*ras* (16), *bcl*2 (17–19), *c-kit* (20), VEGF gene (21) and HIF 1α (22), as well as in fragile X-syndrome (23) and other trinucleotide repeat sequences (24), the retinoblastoma susceptibility gene (25), the chicken β-globin gene (26) and the insulin gene (27). G-rich sequences are especially abundant in gene promoter regions (8) and there is an overabundance of G-rich sequences in the regulatory regions of muscle-specific genes (28).

For intramolecular quadruplexes, the four G-tracts are separated by loops. These are of various lengths and can be as short as a single nucleotide (29–31). Genomic searches (7,9) have revealed many G-rich sequences which may be able to adopt these structures, the most common of which are successive G-tracts that are separated by single T or A residues. The loops can be arranged in several different ways; double-chain reversal (propeller) loops link two adjacent parallel strands (32), while edgewise or diagonal loops link two antiparallel strands (33). Some structures contain both edge-wise and propeller loops (34–36). In the all-parallel (propeller) structures, the nucleotides are in the *anti* conformation, while the other structures have different combinations of *anti* or *syn* glycosidic bonds (3,4). It is known that loop length and sequence affect quadruplex stability and structure (29,37–40). Sequences with single nucleotide loops between the G_3 tracts only adopt a parallel structure, while longer loops can also adopt an antiparallel arrangement of the strands. Quadruplex stability is also affected by the sequence of the loops (39–41), and the bases that flank the quadruplex (42–44).

There is considerable variation in quadruplex structure, depending on the DNA sequence and the ionic conditions. The biological function of quadruplexes may well depend on the folded conformation that is adopted, especially if this involves interaction with specific proteins. Such an effect has been suggested for the NHE element of the c-myc promoter, which can in principle adopt multiple conformations. Since the loops can have a considerable

*To whom correspondence should be addressed. Tel: +44 23 8059 4374; Fax: +44 23 8059 4459; Email: k.r.fox@soton.ac.uk

effect on quadruplex folding and stability, we have examined how changes in loop length affect quadruplex properties. One very stable intramolecular quadruplex contains four G_3 tracts that are linked by single T residues (30,41,45) and this is known to be an inhibitor of HIV integrase. We have used variations on this sequence to examine the importance of loop length on quadruplex folding and stability. In this study, we have systematically replaced each of the single T loops with T_4 and have used CD, fluorescence melting, 1D-NMR, gel electrophoresis and kinetic studies to examine the effect of loop length and position on quadruplex folding and stability.

MATERIAL AND METHODS

Oligonucleotides

All oligonucleotides were synthesized on an Applied Biosystems ABI 394 automated DNA/RNA synthesiser on the 0.2 μmole scale using the standard cycles of acid-catalysed detritylation, coupling, capping and iodine oxidation procedures. Phosphoramidite monomers and other reagents were purchased from Applied Biosystems, Proligo and Link Technologies. The sequences of the oligonucleotides used in this work are shown in Table 1. Fluorescently labelled oligonucleotiodes were used in all the experiments. These were labelled at the 5′-end with 6-amidohexylfluorescein (FAM), and at the 3′-end with dabcyl using C7 dabcyl cpg (Link Technologies). Oligonucleotides were purified by gel filtration using Nap10 columns (GE Healthcare) and analysed by gel electrophoresis. The bases adjacent to the fluorophore and quencher were the same (T) for all the oligonucleotides to avoid any differences in their effects on quadruplex formation and stability.

Fluorescence melting studies

The thermal melting temperatures of the quadruplexes were determined using the fluorescence melting technique that we have developed (46) and have used previously for assessing the stability of related quadruplexes (39,41,44,47). When the sequence adopts a folded structure the quencher and fluorophore are in close proximity and the fluorescence is quenched. When the structure melts, these groups become separated and there is a large increase in fluorescence. Since the fluorophore and quencher are anchored on relatively long aliphatic tethers the quenching does not depend on the quadruplex topology and the fluorescence is quenched for both parallel and antiparallel complexes. Fluorescence melting experiments were conducted in a Roche LightCycler as previously described (39,41,44,46,47) in a total reaction volume of 20 μl. Oligonucleotides (final concentration 0.25 μM) were prepared in 10 mM lithium phosphate pH 7.4, which was supplemented with various concentrations of potassium chloride or sodium chloride. The LightCycler has one excitation source (488 nm) and the changes in fluorescence were measured at 520 nm. For several of the oligonucleotides initial experiments revealed that there was considerable hysteresis between the heating and annealing profiles when the temperature was changed at $0.2°C.s^{-1}$, indicating that the process was not at thermodynamic equilibrium. Melting experiments were therefore performed at a much slower rate of heating and cooling ($0.2°C.min^{-1}$) by changing the temperature in 1°C steps, leaving the samples to equilibrate for 5 min at each temperature before recording the fluorescence. Under these conditions, no hysteresis was observed (except for some experiments with G_3T_4). In a typical experiment, the oligonucleotides were first denatured by heating to 95°C for 5 min. They were then annealed by cooling to 30°C at $0.2°C.min^{-1}$ and melted by heating to 95°C at the same rate. The fluorescence was recorded during both the annealing and melting steps. In some instances, the formation of intramolecular or intermolecular complexes was examined by determining the melting curves using a range of oligonucleotide concentrations (0.1–10 μM). Melting temperatures (T_m values) were determined from the first derivatives of the melting profiles using the Roche LightCycler software.

Table 1. Sequences of the quadruplex-forming oligonucleotides used in this work

Name	Sequence						
	Loop 1		Loop 2		Loop 3		
G_3T	d-F-TGGG	T	GGG	T	GGG	T	GGGT-Q
G_3T-T_4-T	d-F-TGGG	T	GGG	TTTT	GGG	T	GGGT-Q
G_3T_4-T-T	d-F-TGGG	TTTT	GGG	T	GGG	T	GGGT-Q
G_3T_4-T-T_4	d-F-TGGG	TTTT	GGG	T	GGG	TTTT	GGGT-Q
G_3T_4-T_4-T	d-F-TGGG	TTTT	GGG	TTTT	GGG	T	GGGT-Q
G_3T_4	d-F-TGGG	TTTT	GGG	TTTT	GGG	TTTT	GGGT-Q

F = FAM; Q = dabcyl.

Thermodynamic and kinetic analysis

T_m values were obtained from the maxima of the first derivatives of the melting profiles using the LightCycler software or, together with ΔH, from van't Hoff analysis of the melting profiles using FigP for Windows. The fraction folded was calculated as previously described (48) from the difference between the measured fluorescence and the upper and lower baselines. All reactions were performed at least twice and the calculated T_m values usually differed by <0.5°C with a 5% variation in ΔH. Since $\Delta G = 0$ at the T_m, ΔS was estimated as $\Delta H/T_m$. Values for ΔG at 310 K were then estimated from $\Delta G = \Delta H - T\Delta S$. The van't Hoff analysis assumes that ΔH is independent of temperature (i.e. $\Delta C_p = 0$), that the reaction is only a two-step process (i.e. that there are no significant reaction intermediates) and that there is only one folded form of the quadruplex. The number of specifically bound monovalent cations (Δn), was calculated from the slopes of plots of ΔG against $\log[M^+]$ as previously described (30,49).

Hysteresis between the melting and annealing profiles occurs when the reaction is not at thermodynamic equilibrium as a result of the slow folding and/or unfolding kinetics. Individual folding (k_1) and unfolding

(k_{-1}) rate constants can be derived from this hysteresis as previously described (47,48,50,51).

Temperature jump kinetics

The kinetics of quadruplex unfolding were also determined by measuring the rate of change of fluorescence after rapidly increasing the temperature (47,52). The quadruplexes were equilibrated at a temperature around the T_m, which was then rapidly increased by 5°C at the fastest rate on the LightCycler (20°C.s^{-1}). This temperature change causes the quadruplex to partially unfold, moving along the melting curve. Although the theoretical dead-time under these conditions is only 0.25 s, all fluorescence changes that occurred in the first 2 s were ignored, during equilibration to the new temperature. Successive temperature-jumps were then recorded on the same sample by further increasing the temperature by 5°C. Each experiment was repeated at least twice. The time-dependent changes in fluorescence were fitted by an exponential function $F_t = F_f \times (1 - e^{-kt}) + F_0$, using SigmaPlot 10, where F_t is fluorescence at time t, F_0 is the initial fluorescence and F_f is total change in fluorescence (the final fluorescence is $F_f + F_0$). The relaxation rate constant (k) obtained from this analysis is equal to the sum of the folding (k_1) and unfolding (k_{-1}) rate constants. Arrhenius plots of $\ln(k)$ against $1/T$ were constructed from these data and used to estimate the activation energy E_a and pre-exponential factor A [$k = A \times \exp(-E_a/RT)$].

Gel electrophoresis

Non-denaturing gel electrophoresis was performed using 14% polyacrylamide gels, which were run in TBE buffer that had been supplemented with 20 mM KCl. Bands in the gels were visualised under UV light. The oligonucleotide concentration was 20 μM.

Circular dichroism

CD spectra were measured on a Jasco J-720 spectropolarimeter as previously described (39). Oligonucleotide solutions (5 μM) were prepared in 10 mM lithium phosphate pH 7.4, containing either 200 mM potassium chloride or 200 mM sodium chloride. The samples were heated to 95°C and annealed by slowly cooling to 15°C over a period of 12 h. Spectra were recorded between 220 and 320 nm in 5 mm path length cuvettes. Spectra were averaged over 10 scans, which were recorded at 100 nm.min^{-1} with a response time of 1 s and a bandwidth of 1 nm. A buffer baseline was subtracted from each spectrum and the spectra were normalized to have zero ellipticity at 320 nm.

Proton NMR

One-dimensional ^{1}H NMR experiments were performed on a Varian Inova 600 MHz spectrometer. Oligonucleotides were prepared in 200 mM potassium phosphate pH 7.4 and were annealed by heating to 95°C before slowly cooling to 15°C. 300 μl of the oligonucleotide sample was mixed with 20 μl D_2O and placed in a Shigemi NMR tube. The final strand concentration was 100 μM. 1D proton NMR spectra were recorded at 25°C with a sweep width of 25 p.p.m., WATERGATE water suppression, an acquisition time of 0.5 s and 32 k scans. Data were processed using VNMR software (Varian Inc.) with zero filling and resolution enhancement.

RESULTS

A variety of physical techniques were used to examine the folding, stability and kinetics of the intramolecular quadruplexes that are formed by sequences containing four G_3 tracts separated by either single T or T_4 loops, in different combinations. The sequences of these oligonucleotides are shown in Table 1.

Circular dichroism

Intramolecular quadruplexes can adopt a variety of different topologies in which the strands run in different orientations with lateral, edgewise or diagonal loops. Circular dichroism has frequently been used to indicate whether these fold in a parallel or antiparallel configuration (43,53,54). Parallel quadruplexes, in which the glycosidic bonds are all *anti*, display a positive CD signal around 265 nm, with a negative peak at 240 nm. In contrast, antiparallel topologies, with both *syn* and *anti* bonds, exhibit a positive signal at around 295 nm, with a negative signal or shoulder around 260 nm. CD spectra for these oligonucleotides, in the presence of sodium or potassium ions, are shown in Figure 1 [other studies with related sequences have shown that the fluorophores do not affect the CD spectra (55)].

In the presence of potassium (Figure 1) all the sequences, except G_3T_4 show CD spectra with a positive peak around 265 nm and a minimum around 240 nm, which is typical of the parallel configuration. In contrast, G_3T_4 displays a positive peak at 295 nm, indicative of an antiparallel topology. Quadruplexes with single nucleotide loops are thought to be only able to form 'propeller-type' fold-back loops generating parallel-stranded complexes, while longer T_4 loops can form lateral, edgewise or diagonal loops. These CD spectra suggest that the presence of only one single T loop is sufficient to induce the formation of a parallel-stranded structure and that the complexes only adopt an antiparallel arrangement when all the loops are longer. In general, these CD spectra were independent of the potassium concentration in the range 20–200 mM K^+, though pronounced changes were observed for G_3T_4 (inset to Figure 1a). For this sequence a secondary peak is visible around 260 nm at low potassium ion concentrations, which disappears as the potassium ion concentration is increased; this is accompanied by an increase in the peak at 295 nm. The presence of isoelliptic points in these spectra suggests that this sequence may adopt two distinct structural forms in the presence of low or high potassium ion concentrations.

In the presence of sodium ions, the CD spectra for G_3T, G_3T-T_4-T and G_3T_4-T-T are again typical of a parallel topology, with peaks around 265 nm (Figure 1b). However, the addition of a second T_4 loop results in spectra with

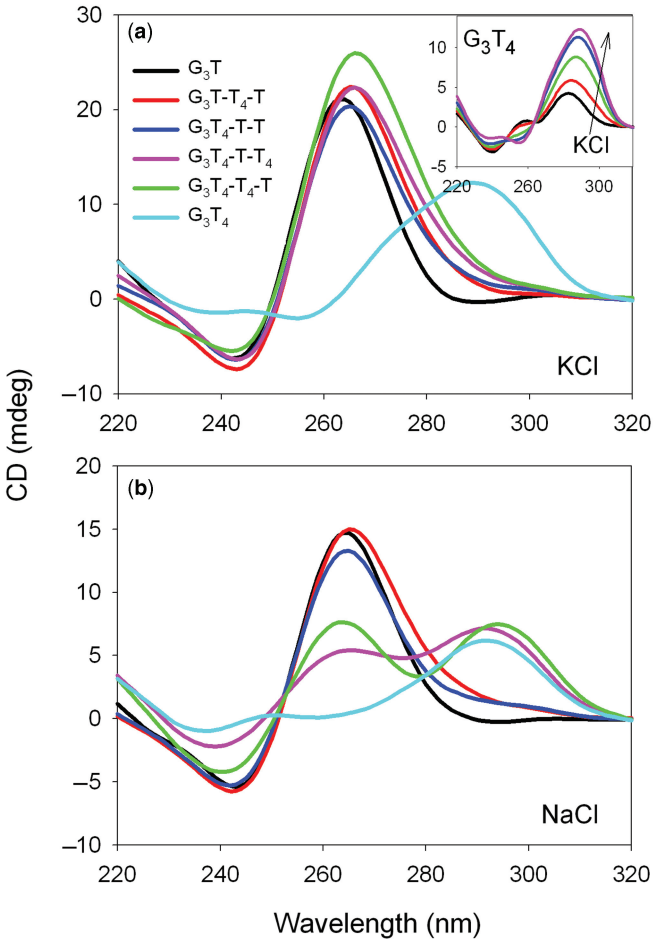

Figure 1. CD spectra of the fluorescently-labelled quadruplex-forming oligonucleotides in the presence of 10 mM lithium phosphate pH 7.4 containing 200 mM KCl (**a**) or 200 mM NaCl (**b**). G_3T, black; G_3T-T_4-T, red; G_3T_4-T-T, blue; G_3T_4-T-T_4, pink; G_3T_4-T_4-T, green; G_3T_4, cyan. The inset to the upper panel shows the CD spectrum of G_3T_4 in the presence of different concentrations of KCl: black 1 mM; red, 5 mM; green 20 mM; blue 50 mM; pink, 200 mM.

equal-sized peaks at 265 nm and 295 nm. It has been suggested that sodium ions promote the formation of antiparallel topologies and it is possible that the two longer T_4 loops are laterally arranged, while the single T loop is in a fold-back arrangement. This mixed spectrum could indicate the co-existence of parallel and antiparallel topologies in solution, but a hybrid structure containing both *syn* and *anti* bonds seems more likely; this will be considered further in the Discussion. The spectrum of G_3T_4 is similar in the presence of sodium and potassium ions, with a peak at 295 nm, suggesting an antiparallel topology.

Gel mobility

We further compared the global structures of these sequences by examining their mobilities in polyacrylamide gels that had been supplemented with 20 mM KCl (Figure 2). Each of the sequences ran as a single band, with the exception of G_3T_4 which is smeared, possibly

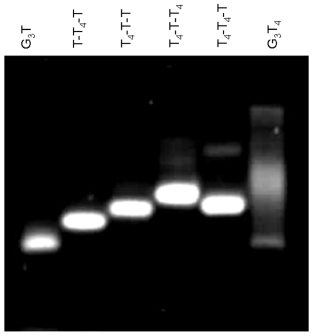

Figure 2. Mobility of the quadruplex-forming oligonucleotides on a 14% polyacrylamide gel supplemented with 20 mM KCl.

because this sequence is less stable under these conditions ($T_m \sim 40°C$, see below). G_3T has the greatest mobility, as expected as it has the lowest molecular weight. Surprisingly we find that G_3T_4-T-T has a lower mobility than G_3T-T_4-T and similarly G_3T_4-T-T_4 is slower than G_3T_4-T_4-T. It appears that the presence of a single T in the central loop reduces the mobility. This will be considered in the Discussion.

Imino proton NMR spectra

One of the defining features of structures that contain G-quartets is the appearance of imino proton resonances between 10.5 and 12.0 p.p.m. in NMR spectra (56). Examination of this region of NMR spectra has often been used to assess whether the sequence adopts a unique structure (20,34,36,56) and the presence of multiple or ill-defined peaks is evidence for the existence of multiple structures. The imino proton spectra for each of these sequences are shown in Figure 3. It can be seen that the spectra of G_3T, G_3T-T_4-T, G_3T_4-T-T and G_3T_4-T-T_4 display between 10 and 12 well-resolved and sharp peaks, indicative of well-defined structures. In the cases where 10 or 11 peaks are resolved, the intensities indicate that one or two imino protons have degenerate chemical shifts. Hence, the number of hydrogen-bonded imino protons is 12, as expected for three stacked G-quartets. G_3T_4-T_4-T also shows 12 major peaks, though the spectrum contains some minor peaks, which might indicate the presence of a small amount of a second structure. In contrast, the imino proton spectrum of G_3T_4 shows multiple peaks confirming that it adopts more than one stable conformation.

Fluorescence melting curves

Representative fluorescent melting curves for these sequences are shown in Figure 4 in the presence of potassium and sodium ions. The T_m values at different ionic strengths, along with the calculated values for ΔH, are shown in Table 2. The samples were melted and annealed at $0.2°C.min^{-1}$; no hysteresis was observed at this rate of temperature change (except for G_3T_4 at low ionic strengths). The melting temperatures were all independent of concentration (between 0.1 and 10 μM; Supplementary material Figure 1) confirming that these oligonucleotide sequences form intramolecular

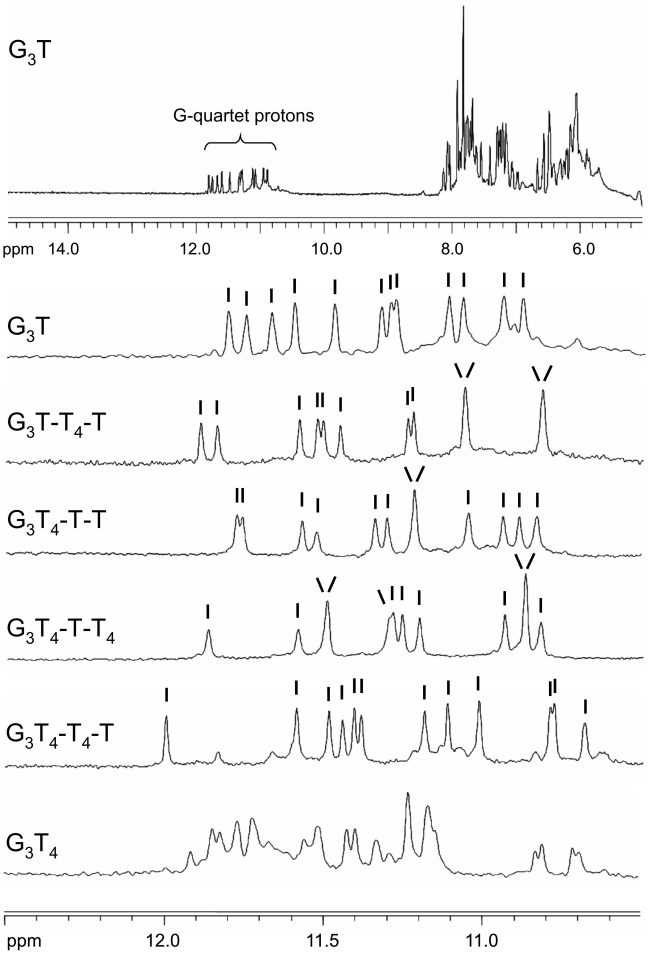

Figure 3. 1D imino proton NMR spectra of the quadruplex-forming oligonucleotides. The samples (100 μM) were prepared in 200 mM potassium phosphate pH 7.4. The top panel shows the 1D-NMR spectrum for G_3T between 5 and 15 p.p.m., while the other panels show the imino proton region for each oligonucleotide. The individual peaks are indicated.

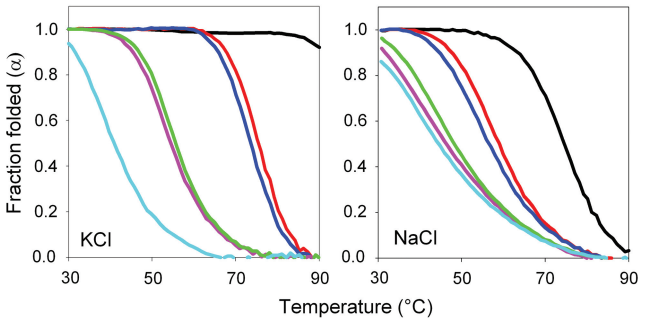

Figure 4. Fluorescence melting profiles for the quadruplex-forming oligonucleotides. The reactions were performed in 10 mM lithium phosphate pH 7.4 containing either 20 mM KCl (left hand panel) or 200 mM NaCl (right hand panel). The temperature was changed at 0.2°C.min^{-1}. The curves show the fraction folded (α) as a function of temperature, calculated as described in the Methods section. G_3T, black; G_3T-T_4-T, red; G_3T_4-T-T, blue; G_3T_4-T-T_4, pink; G_3T_4-T_4-T, green; G_3T_4, cyan.

(not intermolecular) complexes. As expected, all the complexes are more stable in potassium than sodium ions. G_3T is the most stable and, in the presence of potassium, substituting a T_4 loop instead of a loop with a single T decreases the T_m by about 20°C, irrespective of whether the replacement is in a central (G_3T-T_4-T) or peripheral loop (G_3T_4-T-T), though G_3T-T_4-T is about 2–3°C more stable than G_3T_4-T-T. Replacing a second T loop with T_4 causes a further 20°C decrease in T_m and G_3T_4-T_4-T is about 2–4°C more stable than G_3T_4-T-T_4. In each case, the sequence with a single T in the central loop is slightly less stable than the equivalent sequence with T_4 in the same position. Replacing all three single T loops with T_4 decreases the T_m by a further 10°C, though the melting and annealing curves with this sequence show hysteresis at low ionic strengths and the melting (but not the annealing) profiles are biphasic.

The relative order of stability is the same in the presence of sodium ions (Supplementary material Table 1). Replacing one T loop with T_4 decreases the T_m by 15–20°C, and a second substitution causes a further 10°C decrease. Replacing all three loops with T_4 does not affect the stability any further and G_3T_4 has a similar T_m to G_3T_4-T_4-T and G_3T_4-T-T_4. As seen with potassium, sequence isomers with a central T_4 loop are slightly more stable than those with a central T loop (i.e. G_3T_4-T_4-T > G_3T_4-T-T_4 and G_3T-T_4-T > G_3T_4-T-T).

ΔH values for the quadruplex single-strand transition in the presence of potassium were derived from these melting profiles by van't Hoff analysis, assuming that the reaction is a two-state equilibrium, and the values are shown in Table 2. These are typical of those for similar quadruplexes and show a general decrease in ΔH as the overall loop length increases. As previously reported for other quadruplexes, ΔH increases with ionic strength, consistent with the presence of specific cation binding sites within the quadruplex (30). The slopes of plots of ΔG against log[M^+] can be used to determine the stoichiometry of cation binding (30) yielding values of Δn (the difference between the number of ions bound in the folded and unfolded states) and the values of Δn in the presence of potassium are listed in Table 2. For an antiparallel structure containing three stacked G-quartets, Δn would be expected to be either two (the number of potassium ions located between the stacked quartets) or four (including two more ions that may be coordinated between the loops and the terminal quartets). A value of two seems more likely for a parallel topology with single nucleotide loops, in which the loops do not interact with the terminal quartets. The values of Δn are between two and three for all the complexes that contain at least one loop with a single T residue, though there is a steady increase in this value with increased numbers of T_4 loops, which will be considered further in the Discussion. Δn is larger for G_3T_4, consistent with the suggestion that it adopts a different topology, though this value may not be accurate as there is some hysteresis in its melting profiles at low potassium concentrations and the NMR data suggest that it adopts more than one conformation.

Table 2. T_m and ΔH values for the fluorescently labelled quadruplex-forming oligonucleotides, determined in the presence of 10 mM lithium phosphate pH 7.4 containing different concentrations of KCl. The samples were heated and cooled at a rate of 0.2°C.min^{-1}

[KCl] mM	G_3T		G_3T-T_4-T		G_3T_4-T-T		G_3T_4-T-T_4		G_3T_4-T_4-T		G_3T_4	
	T_m°C	ΔH kJ.mol^{-1}	T_m°C	ΔH kJ.mol^{-1}	T_m°C	ΔH kJ.mol^{-1}	T_m°C	ΔH kJ.mol^{-1}	T_m°C	ΔH kJ.mol^{-1}	T_m°C	ΔH kJ.mol^{-1}
0	46.6											
0.1	57.2	−242 ± 4	37.7									
1	73.5	−271 ± 5	53.8	−227 ± 7	51.3	−208 ± 7						
5	85.7	−275 ± 5	65.3	−259 ± 11	63.4	−250 ± 15						
10			70.7	−266 ± 9	67.3	−258 ± 9	46.3	−184 ± 13	48.1	−205 ± 5		
20			75.1	−267 ± 7	73.1	−262 ± 10	52.5	−207 ± 3	54.1	−227 ± 11	44.5/37.6*	
50			81.4	−284 ± 7	79.8	−275 ± 8	59.5	−225 ± 13	60.5	−246 ± 8	47.0/51.0*	−234 ± 11
100			87.5		84.6		65.3	−247 ± 8	67.1	−269 ± 13	56.3	−266 ± 10
200							72.8	−256 ± 9	74.2	−276 ± 10	63.3	−293 ± 9
Δn	2.13 ± 0.10		2.29 ± 0.11		2.31 ± 0.16		2.75 ± 0.11		2.89 ± 0.12		4.01 ± 0.16	

*Indicates a biphasic melting profile. All reactions were performed at least twice and the calculated T_m values usually differed by <0.5°C. ΔH values were typically calculated for melting profiles for which the T_m was between 40°C and 80°C. Missing values at low concentrations of KCl correspond to complexes for which the T_ms were too low to measure (<30°C), while those at high ionic strengths (especially G_3T) were too stable (T_m > 85°C).

Kinetics of quadruplex formation

Hysteresis. The fluorescence melting experiments shown in Figure 4 were performed at a rate of temperature change of 0.2°C.min^{-1} and only G_3T_4 showed hysteresis between the melting and annealing profiles. On increasing the rate to 2°C.min^{-1} there was a 7–10°C hysteresis for the sequences with two T_4 loops in the presence of potassium, though the melting and annealing profiles were identical for the sequences with single T_4 loops. The sequences with single T_4 loops only displayed hysteresis when the rate of heating was increased to 12°C.min^{-1}, while the melting and annealing curves for G_3T were always superimposable. Representative heating and annealing curves at different rates of heating and cooling in the presence of 20 mM potassium are shown in Supplementary material Figure 2 and the different T_m values are summarized in Supplementary Table 1. No hysteresis was observed for any of these sequences in the presence of sodium at even the fastest rate of heating and cooling. Differences between the melting and annealing curves arise because the reaction is not at thermodynamic equilibrium and indicate that either the folding or the unfolding process is slow. The folding (k_1) and unfolding (k_{-1}) rate constants for the unimolecular folding reaction can be obtained by analysis of these data as previously described (47,48). Figure 5a shows the melting and annealing profiles for G_3T_4-T-T and G_3T_4-T-T_4, determined at 12°C.min^{-1} and 2°C.min^{-1}, respectively, while similar plots for G_3T-T_4-T and G_3T_4-T_4-T are included in Supplementary material, Figure 3. Figure 6 shows Arrhenius plots for the folding and unfolding rates constructed from these data for G_3T-T_4-T and G_3T_4-T_4-T (Figure 6a) and G_3T_4-T-T and G_3T_4-T-T_4 (Figure 6b). The kinetic parameters derived from these Arrhenius plots are presented in Table 3. Several factors are apparent from these kinetic data. Firstly, the association reaction shows unusual temperature dependence, with an apparent negative activation energy, i.e. the reaction is faster a lower temperatures. This has been noted by others and is consistent with the reaction occurring by a nucleation-zipper mechanism (47,48). Secondly, the data for G_3T_4-T_4-T are very similar to G_3T_4-T-T_4 and G_3T_4-T-T is similar to G_3T-T_4-T, suggesting that the distribution of the different loops is less important than their length. Thirdly, the unfolding parameters are very similar for all four oligonucleotides, while the folding parameters vary according to the loop lengths. For the association reaction both ln(A) and E_a are less negative for the complexes with longer loops. This kinetic analysis was not performed for G_3T as it showed no hysteresis and for G_3T_4 as the melting and annealing curves were biphasic.

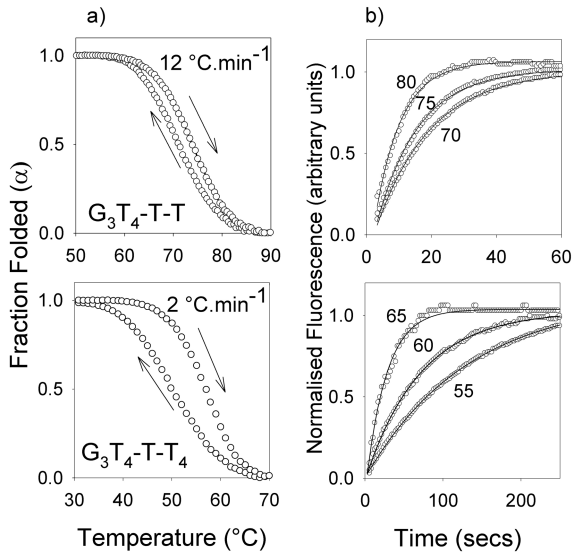

Figure 5. (**a**) Hystersis between the melting and annealing profiles for G_3T_4-T-T (upper panel, with a temperature change of 12°C.min^{-1}) and G_3T_4-T-T_4 (lower panel, with a temperature change of 2°C.min^{-1} in the presence of 10 mM lithium phosphate pH 7.4 containing 20 mM KCl. (**b**) temperature-jump relaxation profiles for G_3T_4-T-T (upper panel) and G_3T_4-T-T_4 (lower panel. The traces show the rate of approach to a new equilibrium following a rapid 5°C increase in temperature to the value shown. The profiles have been normalized to show the fractional change in fluorescence with time.

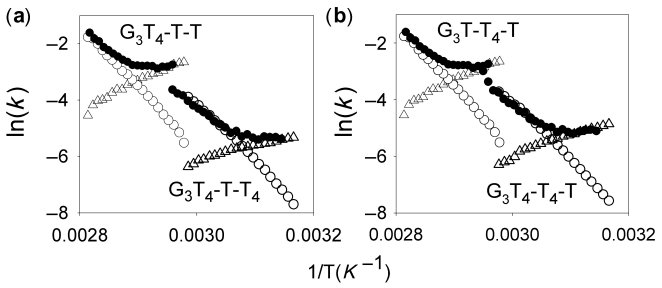

Figure 6. Arrhenius plots showing the temperature dependence of the kinetic parameters for G_3T_4-T-T and G_3T_4-T-T_4 (**a**) and G_3T-T_4-T and G_3T_4-T_4-T (**b**). Open symbols were derived from the hysteresis between the melting and annealing profiles; k_{-1}, open circles; k_1, open triangles. Filled circles show the time constants obtained from the temperature-jump experiments ($k_1 + k_{-1}$).

Table 3. Kinetic parameters for folding (k_1) and unfolding (k_{-1}) of the quadruplex-forming oligonucleotides determined from analysis of the hysteresis between melting and annealing curves

Sequence	k_1		k_{-1}	
	E_a (kJ mol1^{-1})	ln (A) s^{-1}	E_a (kJ mol1^{-1})	ln (A) s^{-1}
G_3T	-	-	-	-
G_3T-T_4-T	-93 ± 2	-36 ± 1	182 ± 3	60 ± 1
G_3T_4-T-T	-88 ± 3	-34 ± 1	178 ± 2	58 ± 1
G_3T_4-T-T_4	-48 ± 4	-24 ± 1	173 ± 2	58 ± 1
G_3T_4-T_4-T	-59 ± 2	-27 ± 1	174 ± 2	59 ± 1
G_3T_4	-	-	-	-

The experiments were performed in 10 mM lithium phosphate pH 7.4 containing 20 mM potassium chloride. E_a is the activation energy (kJ.mol^{-1}) and A is the pre-exponential factor from the equation $k = Ae^{(-Ea/RT)}$. No values are presented for G_3T as it does not show any hysteresis, or G_3T_4 as more than one folded configuration exists in solution.

Temperature-jump kinetics. In order to confirm the kinetic data obtained from the hysteresis experiments we performed temperature-jump relaxation kinetics on these complexes. In this technique, the temperature of the complex (maintained around the T_m) is rapidly increased (by 5°C) and the time-dependent changes in fluorescence are recorded as the reaction relaxes to a new equilibrium. Representative temperature-jump relaxation profiles for these complexes are shown in Figure 5b and reveal a slow time-dependent relaxation to the new equilibrium, which is clearly faster for the complexes with two short loops than the ones with two long loops. The kinetic curves at different temperatures were fitted with single exponential functions and the rate constants obtained are presented as Arrhenius plots in Figure 6. For this unimolecular reaction the apparent rate constant for the relaxation is equal to the sum of the folding and unfolding rate constants ($k_{-1} + k_1$). Although it is not possible to resolve these individual components, at low temperatures the sum is dominated by k_1, while the sum approximates to k_{-1} at high temperatures. It can be seen that there is excellent agreement between the rate constants determined by the two independent methods for each of the sequences, confirming that sequences with longer loops display slower rates of folding with little effect on the rate of unfolding.

DISCUSSION

Topology

Circular dichroism is often used to indicate the folding topology of DNA quadruplexes (20,38,53,54). Antiparallel quadruplexes typically have a positive CD signal at around 295 nm, while parallel quadruplexes display a positive signal around 260 nm. These differences reflect both the arrangements of the strands and the *syn*/*anti* orientations around the glycosidic bonds. Parallel topologies have all-*anti* glycosidic angles, while antiparallel ones have both *syn* and *anti* in varying ratios. However, it is clear that these spectral signatures are not necessarily an indicator of quadruplex folding as some exceptions have been noted (57,58). Nonetheless, CD spectra are useful indicators of changes in global quadruplex configuration for series of related oligonucleotides. In the presence of potassium, all the oligonucleotides that contain at least one single T loop exhibit a similar CD spectrum that is indicative of a parallel topology. It therefore appears that in potassium the presence of only one single T loop, in any position, is sufficient to promote all the other loops to form a fold-back propeller-like structure. In principle, these oligonucleotides could adopt several different folded configurations, yet the NMR and gel electrophoresis experiments suggest that only one predominates. When all three loops contain T_4, there is a dramatic change in the CD spectrum to a form that is consistent with antiparallel folding, though the details are dependent on the ionic strength suggesting that G_3T_4 can adopt multiple configurations. This again is consistent with the NMR and electrophoresis experiments, which suggest the presence of multiple folded forms. Previous studies have suggested that the quadruplex formed by $d(G_3T_4G_3)_2$ adopts an antiparallel hairpin dimer in the presence of both sodium and potassium (59,60).

A similar effect is seen for G_3T, G_3T_4-T-T and G_3T-T_4-T in the presence of sodium ions and these display CD spectra that are consistent with parallel topologies. However, the greater propensity to form antiparallel structures in the presence of sodium is seen with T_4-T_4-T and T_4-T-T_4 loops, which have CD spectra with peaks at both 260 nm and 295 nm. This may indicate the presence of multiple structural forms, but it is more likely due to the formation of a structure that contains both edgewise (T_4) and fold-back (T) loops, as observed with other sequences (34–36).

Stability

The fluorescence melting experiments show that the number of short loops, rather than their position, has the greatest effect on quadruplex stability. In the presence of potassium ions, G_3T is the most stable and in concentrations above 5 mM it does not display a melting transition. Substituting a T_4 into either the first or second loop decreases the T_m by about 20°C, with a further 20°C decrease on introducing a second T_4 substitution. The same effect is seen in the presence of sodium ions though there is only a small decrease in stability on changing the third loop to T_4, consistent with the CD spectra which

show that G_3T_4-T-T_4, G_3T_4-T_4-T and G_3T_4 display some antiparallel characteristics in contrast to all the other oligonucleotides.

It is noticeable that sequences with a single T loop in the central position are less stable and have lower gel mobilities than their sequence isomers with T_4 in this position (i.e. compare T_4-T-T_4 loops with T_4-T_4-T and T_4-T-T with T-T_4-T). It appears that folded structures with a central T_4 loop are more compact and have higher thermal stability. There is then a further decrease in stability when all three loops are composed of T_4, which as noted above adopts a different configuration.

Potassium ion binding

The variation of ΔG with ionic strength allows us to estimate the difference in the number of potassium ions specifically bound to the folded and unfolded structures. This value is close to two for G_3T as expected, since two potassium ions can bind between the three stacked quartets. Although the precise values of Δn should be interpreted with caution, it is noticeable that there is a steady increase in this value as the number of longer loops is increased. The value of Δn is similar for G_3T-T_4-T and G_3T_4-T-T and is lower than for both G_3T_4-T_4-T and G_3T_4-T-T_4. These results suggest that the longer loops are involved in cation binding. The larger value of Δn seen with G_3T_4 may not be significant, as this sequence adopts multiple configurations.

Kinetic analysis

Comparing the kinetic parameters for the sequences with one or two T_4 loops (Table 3) reveals that the unfolding parameters are very similar, while there are clear differences in the folding reaction. Complexes with longer loops have higher (less negative) activation energies for the association reaction and larger values for the pre-exponential factor (which is related to the entropy of the transition state). In comparison, no hysteresis is observed with G_3T and temperature-jump experiments showed a very fast re-equilibration, while G_3T_4 has slower folding and unfolding parameters, though not as slow as G_4T_4 (47). It is clear that the folding of intramolecular structures with only single T loops is fast, and we imagine that when one loop is composed of a single nucleotide the G-tracts on either side rapidly associate, forming a platform to which the other G-tracts can bind. The results with the oligonucleotides containing one or two T_4 loops suggest that the position of the single-base loop has little effect on the kinetics and that the most important factor is the number of longer loops.

It is interesting to note that none of these sequences show any hysteresis in the presence of sodium ions, even though G_3T and those with two single T loops appear to adopt a similar global structure. The higher stability and slower kinetics in the presence of potassium may therefore reflect conformational changes subsequent to the initial folding events (45).

SUPPLEMENTARY DATA

Supplementary Data are available at NAR Online.

ACKNOWLEDGEMENTS

PAR is supported by a research studentship from BBSRC.

Conflict of interest statement. None declared.

REFERENCES

1. Burge,S., Parkinson,G.N., Hazel,P., Todd,A.K. and Neidle,S. (2006) Quadruplex DNA: sequence, topology and structure. *Nucleic Acids Res.*, **34**, 5402–5415.
2. Davis,J.T. (2004) G-quartets 40 years later: From 5′-GMP to molecular biology and supramolecular chemistry. *Angew. Chem. Int. Ed. Engl.*, **43**, 668–698.
3. Phan,A.T., Kuryavyi,V. and Patel,D.J. (2006) DNA architecture: from G to Z. *Curr. Opin. Struct. Biol.*, **16**, 288–298.
4. Simonsson,T. (2001) G-quadruplex DNA structures - Variations on a theme. *Biol. Chem.*, **382**, 621–628.
5. Sen,D. and Gilbert,W. (1990) A sodium-potassium switch in the formation of 4-stranded G4-DNA. *Nature*, **344**, 410–414.
6. Williamson,J.R., Raghuraman,M.K. and Cech,T.R. (1989) Mono-valent cation induced atructure of telomeric DNA - the G-quartet model. *Cell*, **59**, 871–880.
7. Huppert,J.L. and Balasubramanian,S. (2005) Prevalence of quadruplexes in the human genome. *Nucleic Acids Res.*, **33**, 2908–2916.
8. Huppert,J.L. and Balasubramanian,S. (2007) G-quadruplexes in promoters throughout the human genome. *Nucleic Acids Res.*, **35**, 406–413.
9. Todd,A.K., Johnston,M. and Neidle,S. (2005) Highly prevalent putative quadruplex sequence motifs in human DNA. *Nucleic Acids Res.*, **33**, 2901–2907.
10. Sen,D. and Gilbert,W. (1988) Formation of parallel 4-stranded complexes by guanine-rich motifs in DNA and its implications for meiosis. *Nature*, **334**, 364–366.
11. Sundquist,W.I. and Klug,A. (1989) Telomeric DNA dimerizes by formation of guanine tetrads between hairpin loops. *Nature*, **342**, 825–829.
12. Ambrus,A., Chen,D., Dai,J.X., Jones,R.A. and Yang,D.Z. (2005) Solution structure of the biologically relevant G-quadruplex element in the human c-*MYC* promoter. implications for G-quadruplex stabilization. *Biochemistry*, **44**, 2048–2058.
13. Rangan,A., Fedoroff,O.Y. and Hurley,L.H. (2001) Induction of duplex to G-quadruplex transition in the c-myc promoter region by a small molecule. *J. Biol. Chem.*, **276**, 4640–4646.
14. Siddiqui-Jain,A., Grand,C.L., Bearss,D.J. and Hurley,L.H. (2002) Direct evidence for a G-quadruplex in a promoter region and its targeting with a small molecule to repress c-*MYC* transcription. *Proc. Natl Acad. Sci. USA*, **99**, 11593–11598.
15. Simonsson,T., Pecinka,P. and Kubista,M. (1998) DNA tetraplex formation in the control region of c-myc. *Nucleic Acids Res.*, **26**, 1167–1172.
16. Cogoi,S. and Xodo,L.E. (2006) G-quadruplex formation within the promoter of the KRAS proto-oncogene and its effect on transcription. *Nucleic Acids Res.*, **34**, 2536–2549.
17. Dai,J.X., Chen,D., Jones,R.A., Hurley,L.H. and Yang,D.Z. (2006) NMR solution structure of the major G-quadruplex structure formed in the human BCL2 promoter region. *Nucleic Acids Res.*, **34**, 5133–5144.
18. Dai,J.X., Dexheimer,T.S., Chen,D., Carver,M., Ambrus,A., Jones,R.A. and Yang,D.Z. (2006) An intramolecular G-quadruplex structure with mixed parallel/antiparallel G-strands formed in the human BCL-2 promoter region in solution. *J. Am. Chem. Soc.*, **128**, 1096–1098.
19. Dexheimer,T.S., Sun,D. and Hurley,L.H. (2006) Deconvoluting the structural and drug-recognition complexity of the G-quadruplex-forming region upstream of the bcl-2 P1 promoter. *J. Am. Chem. Soc.*, **128**, 5404–5415.

20. Rankin,S., Reszka,A.P., Huppert,J., Zloh,M., Parkinson,G.N., Todd,A.K., Ladame,S., Balasubramanian,S. and Neidle,S. (2005) Putative DNA quadruplex formation within the human c-*kit* oncogene. *J. Am. Chem. Soc.*, **127**, 10584–10589.
21. Sun,D.Y., Guo,K.X., Rusche,J.J. and Hurley,L.H. (2005) Facilitation of a structural transition in the polypurine/polypyrimidine tract within the proximal promoter region of the human VEGF gene by the presence of potassium and G-quadruplex-interactive agents. *Nucleic Acids Res.*, **33**, 6070–6080.
22. De Armond,R., Wood,S., Sun,D.Y., Hurley,L.H. and Ebbinghaus,S.W. (2005) Evidence for the presence of a guanine quadruplex forming region within a polypurine tract of the hypoxia inducible factor 1 alpha promoter. *Biochemistry*, **44**, 16341–16350.
23. Fry,M. and Loeb,L.A. (1994) The fragile-X syndrome $d(CGG)_n$ nucleotide repeats form a stable tetrahelical structure. *Proc. Natl Acad. Sci. USA*, **91**, 4950–4954.
24. Matsugami,A., Okuizumi,T., Uesugi,S. and Katahira,M. (2003) Intramolecular higher order packing of parallel quadruplexes comprising a G:G:G:G tetrad and a G(:A):G(:A):G(:A):G heptad of GGA triplet repeat DNA. *J. Biol. Chem.*, **278**, 28147–28153.
25. Murchie,A.I.H. and Lilley,D.M.J. (1992) Retinoblastoma susceptibility genes contain 5′ sequences with a high propensity to form guanine-tetrad structures. *Nucleic Acids Res.*, **20**, 49–53.
26. Howell,R.M., Woodford,K.J., Weitzmann,M.N. and Usdin,K. (1996) The chicken beta-globin gene promoter forms a novel "cinched" tetrahelical structure. *J. Biol. Chem.*, **271**, 5208–5214.
27. Lew,A., Rutter,W.J. and Kennedy,G.C. (2000) Unusual DNA structure of the diabetes susceptibility locus IDDM2 and its effect on transcription by the insulin promoter factor Pur-1/MAZ. *Proc. Natl Acad. Sci. USA*, **97**, 12508–12512.
28. Yafe,A., Etzioni,S., Weisman-Shomer,P. and Fry,M. (2005) Formation and properties of hairpin and tetraplex structures of guanine-rich regulatory sequences of muscle-specific genes. *Nucleic Acids Res.*, **33**, 2887–2900.
29. Hazel,P., Parkinson,G.N. and Neidle,S. (2006) Topology variation and loop structural homology in crystal and simulated structures of a bimolecular DNA quadruplex. *J. Am. Chem. Soc.*, **128**, 5480–5487.
30. Jing,N.J., Rando,R.F., Pommier,Y. and Hogan,M.E. (1997) Ion selective folding of loop domains in a potent anti-HIV oligonucleotide. *Biochemistry*, **36**, 12498–12505.
31. Phan,A.T., Modi,Y.S. and Patel,D.J. (2004) Propeller-type parallel-stranded G-quadruplexes in the human c-myc promoter. *J. Am. Chem. Soc.*, **126**, 8710–8716.
32. Parkinson,G.N., Lee,M.P.H. and Neidle,S. (2002) Crystal structure of parallel quadruplexes from human telomeric DNA. *Nature*, **417**, 876–880.
33. Wang,Y. and Patel,D.J. (1993) Solution structure of the human telomeric repeat $d[AG_3(T_2AG_3)_3]$ G-tetraplex. *Structure*, **1**, 263–282.
34. Ambrus,A., Chen,D., Dai,J.X., Bialis,T., Jones,R.A. and Yang,D.Z. (2006) Human telomeric sequence forms a hybrid-type intramolecular G-quadruplex structure with mixed parallel/antiparallel strands in potassium solution. *Nucleic Acids Res.*, **34**, 2723–2735.
35. Luu,K.N., Phan,A.T., Kuryavyi,V., Lacroix,L. and Patel,D.J. (2006) Structure of the human telomere in K+ solution: An intramolecular (3+1) G-quadruplex scaffold. *J. Am. Chem. Soc.*, **128**, 9963–9970.
36. Phan,A.T., Luu,K.N. and Patel,D.J. (2006) Different loop arrangements of intramolecular human telomeric (3+1) G-quadruplexes in K+ solution. *Nucleic Acids Res.*, **34**, 5715–5719.
37. Cevec,M. and Plavec,J. (2005) Role of loop residues and cations on the formation and stability of dimeric DNA G-quadruplexes. *Biochemistry*, **44**, 15238–15246.
38. Hazel,P., Huppert,J., Balasubramanian,S. and Neidle,S. (2004) Loop-length-dependent folding of G-quadruplexes. *J. Am. Chem. Soc.*, **126**, 16405–16415.
39. Risitano,A. and Fox,K.R. (2004) Influence of loop size on the stability of intramolecular DNA quadruplexes. *Nucleic Acids Res.*, **32**, 2598–2606.
40. Smirnov,I. and Shafer,R.H. (2000) Effect of loop sequence and size on DNA aptamer stability. *Biochemistry*, **39**, 1462–1468.
41. Risitano,A. and Fox,K.R. (2003) Stability of intramolecular DNA quadruplexes: Comparison with DNA duplexes. *Biochemistry*, **42**, 6507–6513.
42. Guo,Q., Lu,M. and Kallenbach,N.R. (1993) Effect of thymine tract length on the structure and stability of model telomeric sequences. *Biochemistry*, **32**, 3596–3603.
43. Lu,M., Guo,Q. and Kallenbach,N.R. (1992) Structure and stability of sodium and potassium complexes of dT_4G_4 and dT_4G_4T. *Biochemistry*, **31**, 2455–2459.
44. Merkina,E.E. and Fox,K.R. (2005) Kinetic stability of intermolecular DNA quadruplexes. *Biophys. J.*, **89**, 365–373.
45. Jing,N.J., Gao,X.L., Rando,R.F. and Hogan,M.E. (1997) Potassium-induced loop conformational transition of a potent anti-HIV oligonucleotide. *J Biomol. Struct. Dyn.*, **15**, 573–585.
46. Darby,R.A.J., Sollogoub,M., McKeen,C., Brown,L., Risitano,A., Brown,N., Barton,C., Brown,T. and Fox,K.R. (2002) High throughput measurement of duplex, triplex and quadruplex melting curves using molecular beacons and a LightCycler. *Nucleic Acids Res.*, **30**, e39.
47. Brown,N.M., Rachwal,P.A., Brown,T. and Fox,K.R. (2005) Exceptionally slow kinetics of the intramolecular quadruplex formed by the Oxytricha telomeric repeat. *Org. Biomol. Chem.*, **3**, 4153–4157.
48. Mergny,J.L. and Lacroix,L. (2003) Analysis of thermal melting curves. *Oligonucleotides*, **13**, 515–537.
49. Cantor,C.R. and Schimmel,P.R. (1980) *Biophysical Chemistry,* W. H. Freedman and Company, New York.
50. Bernal-Mendez,E. and Leumann,C.J. (2002) Stability and kinetics of nucleic acid triplexes with chimaeric DNA/RNA third strands. *Biochemistry*, **41**, 12343–12349.
51. Rougee,M., Faucon,B., Mergny,J.L., Barcelo,F., Giovannangeli,C., Garestier,T. and Helene,C. (1992) Kinetics and thermodynamics of triple-helix formation - effects of ionic-strength and mismatches. *Biochemistry*, **31**, 9269–9278.
52. James,P.L., Brown,T. and Fox,K.R. (2003) Thermodynamic and kinetic stability of intermolecular triple helices containing different proportions of C^+.GC and T.AT triplets. *Nucleic Acids Res.*, **31**, 5598–5606.
53. Balagurumoorthy,P., Brahmachari,S.K., Mohanty,D., Bansal,M. and Sasisekharan,V. (1992) Hairpin and parallel quartet structures for telomeric sequences. *Nucleic Acids Res.*, **20**, 4061–4067.
54. Balagurumoorthy,P. and Brahmachari,S.K. (1994) Structure and stability of human telomeric sequence. *J. Biol. Chem.*, **269**, 21858–21869.
55. Rachwal,P.A., Brown,T and Fox,K.R. (2007) Effect of G-tract length on the structure and stability of intramolecular DNA quadruplexes. *Biochemistry*, **46**, 3036–3044.
56. Feigon,J., Koshlap,K.M. and Smith,F.W. (1995) H-1 NMR spectroscopy of DNA triplexes and quadruplexes. *Methods Enzymol.*, **261**, 225–255.
57. Dapic,V., Abdomerovic,V., Marrington,R., Peberdy,J., Rodger,A., Trent,J.O. and Bates,P.J. (2003) Biophysical and biological properties of quadruplex oligodeoxyribonucleotides. *Nucleic Acids Res.*, **31**, 2097–2107.
58. Esposito,V., Randazzo,A., Piccialli,G., Petraccone,L., Giancola,C. and Mayol,L. (2004) Effects of an 8-bromodeoxyguanosine incorporation on the parallel quadruplex structure $[d(TGGGT)]_4$. *Org. Biomol. Chem.*, **2**, 313–318.
59. Keniry,M.A., Strahan,G.D., Owen,E.A. and Shafer,R.H. (1995) Solution structure of the Na^+ form of the dimeric guanine quadruplex $[d(G_3T_4G_3)]_2$. *Eur. J. Biochem.*, **233**, 631–643.
60. Strahan,G.D., Keniry,M.A. and Shafer,R.H. (1998) NMR structure refinement and dynamics of the K^+-$[d(G_3T_4G_3)]_2$ quadruplex via particle mesh Ewald molecular dynamics simulations. *Biophys. J.*, **75**, 968–981.